Inorg. Chem. **2007**, *46*, 8524–8532

Lanthanide Diruthenium(II,III) Compounds Showing Layered and PtS-Type Open Framework Structures

Bin Liu,[†] Bao-Long Li,[‡] Yi-Zhi Li,[†] Yu Chen,[†] Song-Song Bao,[†] and Li-Min Zheng*[,†]

State Key Laboratory of Coordination Chemistry, Coordination Chemistry Institute, School of Chemistry and Chemical Engineering, Nanjing University, Nanjing 210093, P. R. China, and Key Laboratory of Organic Synthesis of Jiangsu Province, College of Chemistry and Chemical Engineering, Suzhou University, Suzhou 215123, P. R. China

Received November 14, 2006

Two types of lanthanide diruthenium phosphonate compounds, based on the mixed-valent metal–metal bonded paddlewheel core of $Ru_2(hedp)_2^{3-}$ [hedp = 1-hydroxyethylidenediphosphonate, $CH_3C(OH)(PO_3)_2$], have been prepared with the formulas $Ln(H_2O)_4[Ru_2(hedp)_2(H_2O)_2]\cdot 5.5H_2O$ (**1**·Ln, Ln = La, Ce) and $Ln(H_2O)_4[Ru_2(hedp)_2(H_2O)_2]\cdot 8H_2O$ (**2**·Ln, Ln = La, Ce, Pr, Nd, Sm, Eu, Gd, Tb, Dy, Ho, Er). In both types, each $Ru_2(hedp)_2(H_2O)_2^{3-}$ unit is linked by four Ln^{3+}ions through four phosphonate oxygen (O_P) atoms and vice versa. The geometries of the $\{LnO_{P4}\}$ group, however, are different in the two cases. In **1**·Ln, the geometry of $\{LnO_{P4}\}$ is closer to a distorted plane, and thus a square-grid layer structure is found. In **2**·Ln, the geometry of $\{LnO_{P4}\}$ is better described as a distorted tetrahedron; hence, a unique PtS-type open-framework structure is observed. The channels generated in structures **2**·Ln are filled with water aggregates with extensive hydrogen-bond interactions. The magnetic and electrochemical properties are also investigated.

Introduction

A number of hybrid organic−inorganic materials with open framework or porous structures have been fabricated because of their versatile applications in the fields of catalysis,[1a] gas storage, ion exchange, and molecular recognition.[1b−h] The lanthanide ions with intrinsic chemical, magnetic, and spectroscopic properties are privileged partners for the design of functional molecular entities and materials.[2] The coordination versatility and low stereochemical preference of these ions, however, make specific recognition difficult, and thus, the formation of the extended lanthanide-containing heterometallic frameworks is also difficult. Very few lanthanide−transition metal heterometallic coordination polymers with open-framework structures have been reported so far, most of which were prepared with "unprecedented" structures under hydro- or solvothermal conditions.[3] The design and synthesis of extended lanthanide-containing heterometallic frameworks with desired topologies under mild conditions still remain a great challenge.

* To whom correspondence should be addressed. E-mail: lmzheng@netra.nju.edu.cn. Fax: +86-25-83314502.

[†] Nanjing University.

[‡] Suzhou University.

(1) (a) Kesanli, B.; Lin, W. *Coord. Chem. Rev.* **2003**, *246*, 305−326. (b) Cho, S.-H.; Ma, B.; Nguyen, S. T.; Hupp, J. T.; Albrecht-Schmitt, T. E. *Chem. Commun.* **2006**, 2563. (c) Ockwig, N. W.; Delgado-Friedrichs, O.; O'Keeffe, M.; Yaghi, O. M. *Acc. Chem. Res.* **2005**, *38*, 176−182. (d) Eddaoudi, M.; Moler, D. B.; Li, H.-L.; Chen, B.-L.; Reineke, T. M.; O'Keeffe, M.; Yaghi, O. M. *Acc. Chem. Res.* **2001**, *34*, 319−330. (e) Fletcher, A. J.; Thomas, K. M.; Rosseinsky, M. J. *J. Solid State Chem.* **2005**, *178*, 2491−2510. (f) Moulton, B.; Zaworotko, M. J. *Chem. Rev.* **2001**, *101*, 1629−1658. (g) Uemura, K.; Matsuda, R.; Kitagawa, S. *J. Solid State Chem.* **2005**, *178*, 2420−2429. (h) Pan, L.; Olson, D. H.; Ciemnolonski, L. R.; Heddy, R.; Li, J. *Angew. Chem., Int. Ed.* **2006**, *45*, 616−619. (i) Chen, B.; Liang, C.; Yang, J.; Contreras, D. S.; Clancy, Y. L.; Lobkovsky, E. B.; Yaghi, O. M.; Dai, S. *Angew. Chem., Int. Ed.* **2006**, *45*, 1390−1393.

(2) (a) Bünzli, J.-C. G.; Piguet, C. *Chem. Rev.* **2002**, *102*, 1897−1928. (b) Benelli, C.; Gatteschi, D. *Chem. Rev.* **2002**, *102*, 2369−2387. (c) Plecnik, C. E.; Liu, S.; Shore, S. G. *Acc. Chem. Res.* **2003**, *36*, 499−508. (d) Zhou, Y.; Hong, M.; Wu, X. *Chem. Commun.* **2006**, 135−143. (e) Cutland-Van Noord, A. D.; Kampf, J. W.; Pecoraro, V. L. *Angew. Chem., Int. Ed.* **2002**, *41*, 4668−4670.

(3) (a) Baggio, R.; Garland, M. T.; Moreno, Y.; Peña, O.; Perec, M.; Spodine, E. *J. Chem. Soc., Dalton Trans.* **2000**, 2061. (b) Ren, Y. P.; Long, L. S.; Mao, B. W.; Yuan, Y. Z.; Huang, R. B.; Zheng, L. S. *Angew. Chem., Int. Ed.* **2003**, *42*, 532−535. (c) Zhao, B.; Cheng, P.; Dai, Y.; Cheng, C.; Liao, D.-Z.; Yan, S.-P.; Jiang, Z.-H.; Wang, G.-L. *Angew. Chem., Int. Ed.* **2003**, *42*, 934. (d) Zhao, B.; Cheng, P.; Chen, X.-Y.; Cheng, C.; Shi, W.; Liao, D.-Z.; Yan, S.-P.; Jiang, Z.-H. *J. Am. Chem. Soc.* **2004**, *126*, 3012−3013. (e) Zhao, B.; Chen, X.-Y.; Cheng, P.; Liao, D.-Z.; Yan, S.-P.; Jiang, Z.-H. *J. Am. Chem. Soc.* **2004**, *126*, 15394−15395. (f) Cheng, J. W.; Zhang, J.; Zheng, S. T.; Zhang, M. B.; Yang, G. Y. *Angew. Chem., Int. Ed.* **2006**, *45*, 73−77. (g) Zhang, J.-J.; Sheng, T.-L.; Hu, S.-M.; Xia, S.-Q.; Leibeling, G.; Meyer, F.; Fu, Z.-Y.; Chen, L.; Fu, R.-B.; Wu, X.-T. *Chem.—Eur. J.* **2004**, *10*, 3963−3969.

10.1021/ic0621695 CCC: $37.00
Published on Web 09/12/2007

To produce novel lanthanide−transition metal open frameworks, one strategy is to preorganize a simple building block containing transition metal ions which may serve as an adapted receptor for the lanthanide ions.[2a] This approach has been proven to be successful in the construction of a number of monometallic compounds with high stabilities and large pore sizes.[4] The building block we choose here is a metal−metal-bonded mixed-valent diruthenium diphosphonate $Ru_2(hedp)_2^{3-}$ [hedp = 1-hydroxyethylidenediphosphonate, $CH_3C(OH)(PO_3)_2$] with a paddlewheel structure which has unique electronic and magnetic properties ($S = 3/2$).[5] Compared with the diruthenium tetracarboxylate analogues ($[Ru_2(O_2CR)_4]^+$),[6] the $Ru_2(hedp)_2^{3-}$ unit is negatively charged and can act not only as an acceptor by receiving axial ligands but also as a donor by using the four uncoordinated phosphonate oxygen atoms. It is then an ideal receptor for the lanthanide ions. In this paper, we report that the simultaneous assembly of $Ru_2(hedp)_2^{3-}$ and $Ln(NO_3)_3$ (Ln = La, Ce, Pr, Nd, Sm, Eu, Gd, Tb, Dy, Ho, Er) in an aqueous solution leads to the formation of two types of novel Ln−Ru_2 compounds with formulas of $Ln(H_2O)_4[Ru_2(hedp)_2(H_2O)_2]\cdot 5.5H_2O$ (**1**·Ln) and $Ln(H_2O)_4[Ru_2(hedp)_2(H_2O)_2]\cdot 8H_2O$ (**2**·Ln). Compounds **1**·Ln (Ln = La, Ce) have a square-grid layer structure, while compounds **2**·Ln (Ln = La, Ce, Pr, Nd, Sm, Eu, Gd, Tb, Dy, Ho, Er) possess a PtS-type open-framework structure. As far as we are aware, these are the first examples of Ln−Ru_2 heterometallic compounds containing metal−metal bonded paddlewheel cores of Ru_2^{n+}, although a few Ru_2−3d heterometallic coordination polymers have been reported previously.[7]

Experimental Section

Materials and Methods. Compounds $(NH_4)_3[Ru_2(hedp)_2]\cdot 2H_2O$ and $Na_4[Ru_2(hedp)_2Cl]\cdot 16H_2O$ were prepared according to the methods described previously.[5a,b] All the other starting materials were of reagent grade and were obtained from commercial sources without further purification. Elemental analyses were performed in a PE240C elemental analyzer. The infrared spectra were recorded on a VECTOR 22 spectrometer with pressed KBr pellets. Thermal analyses were performed in nitrogen with a heating rate of 20 °C/min on a TGA-DTA V1.1 TA Inst 2100 instrument. The powder XRD patterns were recorded on a Shimadzu XD-3A X-ray diffractometer. Variable-temperature magnetic susceptibility data were obtained on polycrystalline samples (7.46 mg for **1**·La, 7.97 mg for **2**·Ce, 11.86 mg for **2**·Pr, 14.07 mg for **2**·Nd, 10.57 mg for **2**·Sm, 19.31 mg for **2**·Eu, 24.83 mg for **2**·Gd, 23.29 mg for **2**·Tb, 17.98 mg for **2**·Dy, 24.54 mg for **2**·Ho, 18.64 mg for **2**·Er) using a Quantum Design MPMS-XL7 SQUID magnetometer and on polycrystalline samples of **1**·Ce (6.88 mg) and **2**·La (38.24 mg) using a Quantum Design MPMS-XL5 SQUID magnetometer. Diamagnetic corrections were obtained from Pascal's constants.[8]

The electrochemical experiments were carried out using a CHI660C electrochemical workstation (CH Instruments, Shanghai Chenghua Co.) with a conventional three-electrode cell. A Pt plate was used as the auxiliary electrode. The saturated calomel electrode (SCE) electrode was used as the reference electrode. All the potentials were quoted with respect to SCE; a 0.5 M KNO_3 solution was employed as supporting electrolyte. The working electrode was prepared as follows. A glassy carbon (GC) electrode was polished with 0.3 and 0.05 μm Al_2O_3 sequentially. After it was rinsed with doubly distilled water, it was sonicated with absolute ethanol and then with doubly distilled water for about 3 min. The apparent surface area of the GC electrode was 0.07 cm^2; 6 mg of **1**·La or **2**·La and 1 mL of a mixture of 90% H_2O and 10% Nafion (5 wt %) were mixed and sonicated for 1 h. Then, 4 μL of the mixture was cast onto the surface of a GC electrode and dried at the ambient temperature. The working electrodes were obtained and noted as **1**·La/GC or **2**·La/GC electrode. The electrolyte was purged with high-purity nitrogen for at least 10 min prior to experiments to remove the dissolved oxygen, and a nitrogen environment was then kept over the solution in the cell to protect the solution from oxygen. All experiments were performed at room temperature (25 ± 2°C).

Preparation of $La(H_2O)_4[Ru_2(hedp)_2(H_2O)_2]\cdot 5.5H_2O$ (1·La). A solution of $AgNO_3$ (0.0340 g, 0.20 mmol) in 5 mL of water was added to a solution of $Na_4[Ru_2(hedp)_2Cl]\cdot 16H_2O$ (0.1949 g, 0.20 mmol) in 50 mL of water. After it was left standing for 48 h in the dark, a precipitate of AgCl was filtered off. Then a solution of $La(NO_3)_3\cdot 6H_2O$ (0.0868 g, 0.20 mmol) in 10 mL of water was added to the brown filtrate under stirring, and brown amorphous solids deposited immediately. The mixture was kept at room temperature for an extended period of time (greater than 2 months). Eventually, the amorphous solids were completely transformed into red-brown square platelike crystals. Yield: 0.1388 g (75% based on Ru). Sometimes a small quantity of large octahedral block-shaped crystals of compound **2**·La also appeared (<5%), which can be manually separated. Anal. Calcd for $C_4H_{20}O_{20}P_4Ru_2La\cdot 5.5H_2O$: C, 5.04; H, 3.26. Found: C: 4.75; H, 3.84. IR (KBr, cm^{-1}): ν 3385(br, s), 1638(s), 1450(m), 1376(w), 1154(vs), 1148(s), 980(vs), 927(m), 906(m), 821(m), 782(w), 587(vs), 486(s), 453(w), 437(w), 405(w).

(4) For example, see: (a) Chui, S. S.-Y.; Lo, S. M.-F.; Charmant, J. P. H.; Orpen, A. G.; Williams, I. D. *Science* **1999**, *283*, 1148−1150. (b) Chen, B.; Eddaoudi, M.; Hyde, S. T.; O'Keeffe, M.; Yaghi, O. M. *Science* **2001**, *291*, 1021−1023. (c) Cho, S.-H.; Ma, B.; Nguyen, S. T.; Hupp, J. T.; Albrecht-Schmitt, T. E. *Chem. Commun.* **2006**, 2563. (d) Chen, B.; Liang, C.; Yang, J.; Contreras, D. S.; Clancy, Y. L.; Lobkovsky, E. B.; Yaghi, O. M.; Dai, S. *Angew. Chem., Int. Ed.* **2006**, *45*, 1390−1393. (e) Lu, J.; Mondal, A.; Moulton, B.; Zaworotko, M. J. *Angew. Chem., Int. Ed.* **2001**, *40*, 2113−2116. (f) Wang, X.-L.; Qin, C.; Wang, E.-B.; Li, Y.-G.; Su, Z.-M.; Xu, L.; Carlucci, L. *Angew. Chem., Int. Ed.* **2005**, *44*, 5824−5827. (g) Seo, J. S.; Whang, D.; Lee, H.; Jun, S. I.; Oh, J.; Jeon, Y. J.; Kim, K. *Nature* **2000**, *404*, 982−986. (h) Vimont, A.; Goupli, J.-M.; Lavalley, J.-C.; Daturi, M.; Surble, S.; Serre, C.; Millange, F.; Ferey, G.; Audebrand, N. *J. Am. Chem. Soc.* **2006**, *128*, 3218−3227. (i) Chae, H. K.; Siberio-Pérez, D. Y.; Kim, J.; Go, Y.; Eddaoudi, M.; Matzger, A. J.; O'Keeffe, M.; Yaghi, O. M. *Nature* **2004**, *427*, 523−527. (j) Eddaoudi, M.; Kim, J.; Rosi, N.; Vodak, D.; Wachter, J.; O'Keeffe, M.; Yaghi, O. M. *Science* **2002**, *295*, 469−472. (k) Kesanli, B.; Cui, Y.; Smith, M. R.; Bittner, E. W.; Bockrath, B. C.; Lin, W. *Angew. Chem., Int. Ed.* **2005**, *44*, 72. (l) Wang, Z. Q.; Kravtsov, V. C.; Zaworotko, M. J. *Angew. Chem., Int. Ed.* **2005**, *44*, 2877−2880.

(5) (a) Yi, X.-Y.; Zheng, L.-M.; Xu, W.; Feng, S.-H. *Inorg. Chem.* **2003**, *42*, 2827−2829. (b) Yi, X.-Y.; Liu, B.; Jiménez-Aparicio, R.; Urbanos, F. A.; Gao, S.; Xu, W.; Chen, J.-S.; Song, Y.; Zheng, L.-M. *Inorg. Chem.* **2005**, *44*, 4309−4314. (c) Liu, B.; Li, Y.-Z.; Zheng, L.-M. *Inorg. Chem.* **2005**, *44*, 6921−6923. (d) Liu, B.; Yin, P.; Yi, X.-Y.; Song, Y.; Gao, S.; Zheng, L.-M. *Inorg. Chem.* **2006**, *45*, 4205−4213.

(6) (a) Cotton, F. A.; Walton, R. A. *Multiple Bonds between Metal Atoms*, 2nd ed.; Oxford University Press: Oxford, U.K., 1993. (b) Aquino, M. A. S. *Coord. Chem. Rev.* **1998**, *170*, 141. (c) Aquino, M. A. S. *Coord. Chem. Rev.* **2004**, *248*, 102.

(7) (a) Yoshioka, D.; Mikuriya, M.; Handa, M. *Chem. Lett.* **2002**, 1044. (b) Vos, T. E.; Miller, J. S. *Angew. Chem., Int. Ed.* **2005**, *44*, 2. (c) Liao, Y.; Shum, W. W.; Miller, J. S. *J. Am. Chem. Soc.* **2002**, *124*, 9336. (d) Vos, T. E.; Liao, Y.; Shum, W. W.; Her, J.-H.; Stephens, P. W.; Reiff, W. M.; Miller, J. S. *J. Am. Chem. Soc.* **2004**, *126*, 11630.

(8) Kahn, O. *Molecular Magnetism*; VCH Publishers: New York, 1993.

Table 1. Crystallographic Data

	1·La	**1**·Ce	**2**·La	**2**·Ce	**2**·Pr	**2**·Nd
formula	$C_4H_{28}O_{24}P_4Ru_2La$	$C_4H_{28}O_{24}P_4Ru_2Ce$	$C_4H_{36}O_{28}P_4Ru_2La$	$C_4H_{36}O_{28}P_4Ru_2Ce$	$C_4H_{36}O_{28}P_4Ru_2Pr$	$C_4H_{36}O_{28}P_4Ru_2Nd$
M	925.19	926.40	997.26	998.47	999.26	1002.59
cryst syst	monoclinic	monoclinic	monoclinic	monoclinic	monoclinic	monoclinic
space group	$P2_1/n$	$P2_1/n$	$C2/c$	$C2/c$	$C2/c$	$C2/c$
a (Å)	12.955(2)	12.8719(19)	12.6142(13)	12.5865(19)	13.15(6)	12.534(3)
b (Å)	12.858(2)	12.783(2)	14.7918(16)	14.742(2)	14.91(7)	14.703(3)
c (Å)	15.735(3)	15.692(2)	15.7262(13)	15.6938(17)	15.69(7)	15.625(4)
β (deg)	108.098(3)	108.219(3)	94.227(3)	94.163(4)	93.73(5)	94.481(6)
V (Å^3)	2491.4(7)	2452.6(6)	2926.3(5)	2904.3(7)	3071(24)	2870.5(11)
Z	4	4	4	4	4	4
ρ_{calcd} (g/cm^3)	2.467	2.509	2.264	2.284	2.161	2.320
μ(Mo Kα) (mm^{-1})	3.237	3.403	2.775	2.892	2.839	3.149
T (K)	293	293	193	193	293	193
total reflns	12 695	12 974	14 045	14 131	8067	13 883
unique reflns	4524	4791	2674	2657	3012	2627
R_{int}	0.0466	0.0404	0.0216	0.0292	0.064	0.0323
reflns with [$I > 2\sigma(I)$]	3390	3313	2637	2526	2512	2419
F(000)	1796	1800	1956	1960	1964	1968
GOF on F^2	1.001	1.016	1.022	1.001	1.047	0.994
R1, wR2[a]	0.0463,	0.0549,	0.0179,	0.0212,	0.0543,	0.0309,
[$I > 2\sigma(I)$]	0.0928	0.0895	0.0481	0.0498	0.1117	0.0717
(all data)	0.0663,	0.0932,	0.0182,	0.0233,	0.0690,	0.0363,
	0.0972	0.0961	0.0483	0.0512	0.1163	0.0735
$(\Delta\rho)_{max}$, $(\Delta\rho)_{min}$ (e/Å^3)	0.638, −1.277	1.778, −1.466	0.841, −0.500	0.641, −0.459	2.060, −1.519	0.401, −0.827

	2·Gd	**2**·Tb	**2**·Dy	**2**·Ho	**2**·Er
formula	$C_4H_{36}O_{28}P_4Ru_2Gd$	$C_4H_{36}O_{28}P_4Ru_2Tb$	$C_4H_{36}O_{28}P_4Ru_2Dy$	$C_4H_{36}O_{28}P_4Ru_2Ho$	$C_4H_{36}O_{28}P_4Ru_2Er$
M	1015.60	1017.27	1020.85	1023.28	1025.61
cryst syst	monoclinic	monoclinic	monoclinic	monoclinic	monoclinic
space group	$C2/c$	$C2/c$	$C2/c$	$C2/c$	$C2/c$
a (Å)	12.475(2)	12.458(3)	12.475(2)	12.495(18)	12.376(4)
b (Å)	14.6256(19)	14.583(4)	14.6256(19)	14.45(2)	14.501(5)
c (Å)	15.548(3)	15.524(4)	15.548(3)	15.39(2)	15.451(5)
β (deg)	94.518(5)	94.497(4)	94.518(5)	94.146(13)	94.416(3)
V (Å^3)	2828.0(8)	2811.7(13)	2828.0(8)	2771(7)	2764.9(16)
Z	4	4	4	4	4
ρ_{calcd} (g/cm^3)	2.385	2.403	2.398	2.453	2.464
μ(Mo Kα) (mm^{-1})	3.706	3.884	4.003	4.244	4.427
T (K)	193	293	193	293	293
total reflns	13 288	10 808	13 685	7385	7989
unique reflns	2595	3081	2547	2721	2714
R_{int}	0.0504	0.0258	0.0398	0.0532	0.0408
reflns with [$I > 2\sigma(I)$]	2252	2840	2380	1958	2187
F(000)	1984	1988	1992	1996	2000
GOF on F^2	1.000	1.012	1.041	0.981	1.088
R1, wR2[a]	0.0450,	0.0382,	0.0430,	0.0489,	0.0541,
[$I > 2\sigma(I)$]	0.1134	0.0955	0.1345	0.0855	0.1121
(all data)	0.0545,	0.0338,	0.0474,	0.0720,	0.0765,
	0.1167	0.0972	0.1375	0.0892	0.1174
$(\Delta\rho)_{max}$, $(\Delta\rho)_{min}$ (e/Å^3)	0.591, −0.925	0.706, −1.784	0.757, −1.619	1.932, −1.027	0.776, −0.828

[a] $R1 = \sum||F_o| - |F_c||/\sum|F_o|$; $wR2 = [\sum w(F_o^2 - F_c^2)^2/\sum w(F_o^2)^2]^{1/2}$.

Preparation of $Ce(H_2O)_4[Ru_2(hedp)_2(H_2O)_2]\cdot 5.5H_2O$ (1·Ce). This compound can be prepared following the same procedure as that for **1**·La, except $Ce(NO_3)_3\cdot 6H_2O$ is used instead of $La(NO_3)_3\cdot 6H_2O$. In this case, however, **1**·Ce appears as a minor phase with a yield of 0.0043 g (2% based on Ru). The major phase is compound **2**·Ce with a yield of ~68%. Anal. Calcd for $C_4H_{20}O_{20}P_4Ru_2Ce\cdot 5.5H_2O$: C, 5.03; H, 3.25. Found: C, 4.96; H, 3.25. IR (KBr, cm^{-1}): ν 3384(br, s), 1638(s), 1451(m), 1371(w), 1327(w), 1159-(vs), 982(vs), 926(m), 906(m), 822(m), 587(vs), 487(s), 438(w), 409(w).

Preparation of $La(H_2O)_4[Ru_2(hedp)_2(H_2O)_2]\cdot 8H_2O$ (2·La). A mixture of $(NH_4)_3[Ru_2(hedp)_2]\cdot 2H_2O$ (0.1390 g, 0.20 mmol) in a 100 mL aqueous solution of 0.1 M $LiNO_3$ was heated at 100 °C under stirring for 5 h. The resulting brown-red filtrate was diluted to 900 mL (2×10^{-4} M). Then a solution of $La(NO_3)_3\cdot 6H_2O$ (0.0865 g 0.20 mmol) in water (10 mL) was added under stirring. The brown-red clear solution was allowed to stand at room temperature. After one week, brown octahedral block-shaped crystals of **2**·La precipitated as a pure phase. Yield: 0.1356 g (68% based on Ru). Anal. Calcd for $C_4H_{20}O_{18}P_4Ru_2La\cdot 8H_2O$: C, 4.82;

Table 2. Selected Bond Lengths (Å) and Angles (deg) for Compounds **1**·Ln[a]

	1·La	**1**·Ce		**1**·La	**1**·Ce
Ln(1)−O(13A)	2.370(5)	2.359(5)	Ru(1)−O(12)	2.024(5)	2.007(5)
Ln(1)−O(6B)	2.409(5)	2.404(5)	Ru(1)−O(5)	2.028(5)	2.036(5)
Ln(1)−O(3)	2.436(5)	2.431(5)	Ru(1)−O(2)	2.055(5)	2.038(6)
Ln(1)−O(10C)	2.450(5)	2.447(5)	Ru(1)−O(9)	2.060(5)	2.040(5)
Ln(1)−O(19)	2.522(5)	2.523(6)	Ru(1)−O(16)	2.292(4)	2.298(5)
Ln(1)−O(17)	2.561(5)	2.532(6)	Ru(2)−O(11)	2.016(5)	1.994(5)
Ln(1)−O(18)	2.604(5)	2.586(4)	Ru(2)−O(8)	2.044(5)	2.035(5)
Ln(1)−O(20)	2.655(5)	2.659(5)	Ru(2)−O(4)	2.050(5)	2.038(5)
Ru(1)−Ru(2)	2.357(1)	2.350(1)	Ru(2)−O(1)	2.059(5)	2.064(5)
Ru(2)−O(15)	2.341(5)	2.316(5)			
O(13A)−Ln(1)−O(6B)	92.7(2)	92.7(2)	O(19)−Ln(1)−O(17)	139.9(2)	139.8(2)
O(13A)−Ln(1)−O(3)	140.4(2)	140.9(2)	O(13A)−Ln(1)−O(18)	78.5(2)	78.3(2)
O(6B)−Ln(1)−O(3)	86.4(2)	86.2(2)	O(6B)−Ln(1)−O(18)	66.3(2)	66.2(2)
O(13A)−Ln(1)−O(10C)	86.4(2)	86.7(2)	O(3)−Ln(1)−O(18)	135.2(2)	134.7(2)
O(6B)−Ln(1)−O(10C)	156.5(2)	156.2(2)	O(10C)−Ln(1)−O(18)	135.9(2)	136.4(2)
O(3)−Ln(1)−O(10C)	79.6(2)	79.6(2)	O(19)−Ln(1)−O(18)	77.7(2)	77.7(2)
O(13A)−Ln(1)−O(19)	147.5(2)	147.1(2)	O(17)−Ln(1)−O(18)	131.9(2)	131.9(2)
O(6B)−Ln(1)−O(19)	97.6(2)	97.7(2)	O(13A)−Ln(1)−O(20)	75.7(2)	76.1(2)
O(3)−Ln(1)−O(19)	71.3(2)	71.2(2)	O(6B)−Ln(1)−O(20)	131.7(2)	131.5(2)
O(10C)−Ln(1)−O(19)	95.5(2)	95.6(2)	O(3)−Ln(1)−O(20)	131.5(1)	131.2(2)
O(13A)−Ln(1)−O(17)	72.4(2)	72.9(2)	O(10C)−Ln(1)−O(20)	70.8(2)	71.3(2)
O(6B)−Ln(1)−O(17)	77.6(2)	77.5(2)	O(19)−Ln(1)−O(20)	74.4(2)	73.6(2)
O(3)−Ln(1)−O(17)	68.7(2)	68.7(2)	O(17)−Ln(1)−O(20)	137.5(2)	138.3(2)
O(10C)−Ln(1)−O(17)	79.8(2)	79.6(2)	O(18)−Ln(1)−O(20)	65.4(2)	65.4(2)

[a] Symmetry codes: A $x, y-1, z$; B $-x+1/2, y-1/2, -z+1/2$; C $-x+3/2, y-1/2, -z+1/2$.

Table 3. Selected Bond Lengths (Å) and Angles (deg) for Compounds **2**·Ln[a]

	2·La	**2**·Ce	**2**·Pr	**2**·Nd	**2**·Gd	**2**·Tb	**2**·Dy	**2**·Ho	**2**·Er
Ru(1)−O(1)	2.026(2)	2.024(2)	2.070(8)	2.024(3)	2.022(4)	2.018(3)	2.023(4)	1.989(5)	2.009(5)
Ru(1)−O(4)	2.029(2)	2.028(2)	2.019(7)	2.033(3)	2.027(4)	2.029(3)	2.037(4)	2.021(5)	2.020(5)
Ru(1)−O(5A)	2.032(2)	2.033(2)	2.068(8)	2.023(3)	2.021(4)	2.022(3)	2.047(4)	2.017(5)	2.027(5)
Ru(1)−O(2A)	2.037(2)	2.035(2)	2.056(7)	2.042(3)	2.040(4)	2.030(3)	2.045(4)	2.037(5)	2.034(5)
Ru(1)−O(8)	2.300(2)	2.290(2)	2.331(10)	2.284(3)	2.293(5)	2.286(3)	2.271(5)	2.254(5)	2.253(5)
Ru(1)−Ru(1A)	2.356(1)	2.356(1)	2.418(9)	2.351(1)	2.354(1)	2.346(1)	2.360(1)	2.353(3)	2.342(2)
La(1)−O(6)	2.402(2)	2.378(2)	2.532(9)	2.353(3)	2.317(5)	2.294(3)	2.300(4)	2.291(6)	2.278(5)
La(1)−O(3C)	2.464(2)	2.443(2)	2.490(10)	2.393(3)	2.377(4)	2.382(3)	2.363(4)	2.353(5)	2.333(6)
La(1)−O(10)	2.562(2)	2.530(2)	2.208(9)	2.485(3)	2.413(5)	2.413(3)	2.403(5)	2.379(6)	2.389(5)
La(1)−O(9)	2.606(2)	2.582(2)	2.593(9)	2.533(3)	2.476(5)	2.457(3)	2.445(5)	2.398(5)	2.436(5)
O(6B)−La(1)−O(6)	101.0(1)	101.1(1)	106.9(4)	100.3(1)	99.0(2)	99.2(2)	99.2(2)	101.5(2)	99.0(3)
O(6)−La(1)−O(3C)	142.6(1)	142.6(1)	149.3(2)	142.7(1)	143.3(2)	142.6(1)	143.7(2)	143.9(2)	143.6(2)
O(6)−La(1)−O(3D)	74.9(1)	75.1(1)	68.7(3)	74.7(1)	75.0(2)	76.0(1)	75.1(2)	75.2(2)	75.5(2)
O(3C)−La(1)−O(3D)	130.4(1)	130.0(1)	130.8(4)	130.9(1)	130.6(2)	129.6(2)	129.9(2)	128.4(3)	129.5(3)
O(6B)−La(1)−O(10)	71.2(1)	71.5(1)	74.5(2)	71.5(1)	71.9(2)	71.8(1)	72.1(2)	73.8(2)	72.3(2)
O(6)−La(1)−O(10)	80.8(1)	80.8(1)	77.3(2)	81.3(1)	81.1(2)	80.6(1)	80.6(2)	78.7(2)	80.8(2)
O(3C)−La(1)−O(10)	129.5(1)	129.8(1)	127.0(2)	128.7(1)	128.2(2)	129.9(1)	128.5(2)	131.6(2)	128.7(2)
O(3D)−La(1)−O(10)	71.4(1)	71.2(1)	74.9(2)	71.2(1)	71.4(2)	70.9(1)	71.6(2)	70.3(2)	71.3(2)
O(10)−La(1)−O(10B)	135.4(1)	135.8(1)	131.8(4)	137.2(1)	138.0(2)	136.9(2)	137.4(2)	135.9(3)	138.1(3)
O(6B)−La(1)−O(9)	146.7(1)	146.8(1)	137.8(2)	146.6(1)	146.6(2)	147.4(1)	146.4(2)	146.3(2)	146.5(2)
O(6)−La(1)−O(9)	94.2(1)	93.6(1)	96.8(3)	94.4(1)	95.0(2)	94.4(1)	94.5(2)	94.0(2)	94.6(2)
O(3C)−La(1)−O(9)	75.1(1)	75.2(1)	73.1(3)	75.5(1)	75.7(2)	75.2(1)	75.7(2)	74.7(2)	75.4(2)
O(3D)−La(1)−O(9)	70.0(1)	69.9(1)	71.9(3)	70.2(1)	69.8(2)	69.6(1)	69.7(2)	69.1(2)	69.6(2)
O(10)−La(1)−O(9)	141.1(1)	140.9(1)	146.0(2)	140.9(1)	140.7(2)	140.1(1)	140.9(2)	139.2(2)	140.6(2)
O(10B)−La(1)−O(9)	76.3(1)	76.0(1)	76.1(4)	75.1(1)	74.7(2)	75.8(1)	74.6(2)	77.1(2)	74.4(2)
O(9)−La(1)−O(9B)	88.8(1)	89.8(1)	87.7(4)	89.4(2)	89.6(2)	89.7(2)	90.6(2)	89.2(3)	90.6(2)

[a] Symmetry codes: A $-x+3/2, -y+1/2, -z+1$; B $-x+1, y, -z+1/2$; C $x-1/2, y+1/2, z$; D $-x+3/2, y+1/2, -z+1/2$.

H, 3.61. Found: C: 4.66; H, 3.42. IR (KBr, cm^{-1}): ν 3421(br, s), 1637(s), 1450(m), 1388(w), 1367(w), 1125(vs), 974(vs), 937(m), 904(m), 820(m), 578(vs), 485(s).

Preparation of $Ln(H_2O)_4[Ru_2(hedp)_2(H_2O)_2]\cdot 8H_2O$ (2·Ln) (Ln = Ce, Pr, Nd, Sm, Eu, Gd, Tb, Dy, Ho, Er). These compounds were obtained following the method described for **2**·La. Yields: ~70% based on Ru. For **2**·Ce, Anal. Calcd for $C_4H_{20}O_{18}P_4Ru_2Ce\cdot 8H_2O$: C, 4.81; H, 3.61. Found: C: 5.10; H, 3.36. IR (KBr, cm^{-1}): ν 3422(br, s), 1638(s), 1450(m), 1397(w), 1367(w), 1124(vs), 974(vs), 937(m), 905(m), 821(m), 579(vs), 484(s). For **2**·Pr, Anal. Calcd for $C_4H_{20}O_{18}P_4Ru_2Pr\cdot 8H_2O$: C, 4.80; H, 3.60. Found: C: 4.71; H, 3.55. IR (KBr, cm^{-1}): ν 3422(br, s), 1640(s), 1450(m), 1387(w), 1368(w), 1124(vs), 975(vs), 936(m), 905(m), 820(m), 579(vs), 485(s). For **2**·**Nd**, Anal. Calcd for $C_4H_{20}O_{18}P_4Ru_2Nd\cdot 8H_2O$: C, 4.79; H, 3.59. Found: C: 4.76; H, 3.63. IR (KBr, cm^{-1}): ν 3417(br, s), 1640(s), 1450(m), 1387(w), 1368(w), 1126(vs), 976(vs), 935(m), 905(m), 820(m), 580(vs), 485(s). For **2**·Sm, Anal. Calcd for $C_4H_{20}O_{18}P_4Ru_2Sm\cdot 8H_2O$: C, 4.76; H, 3.57. Found: C: 4.74; H, 3.63. IR (KBr, cm^{-1}): ν 3416(br, s), 1644(s), 1450(m), 1389(w), 1369(w), 1129(vs), 976(vs), 933(m), 905(m), 819(m), 581-(vs), 486(s). For **2**·Eu, Anal. Calcd for $C_4H_{20}O_{18}P_4Ru_2Eu\cdot 8H_2O$: C, 4.75; H, 3.56. Found: C: 4.74; H, 3.63. IR (KBr, cm^{-1}):

ν 3417(br, s), 1646(s), 1450(m), 1401(w), 1368(w), 1145(vs), 975-(vs), 928(m), 906(m), 818(m), 581(vs), 484(s). For **2**·Gd, Anal. Calcd for $C_4H_{20}O_{18}P_4Ru_2Gd\cdot 8H_2O$: C, 4.73; H, 3.54. Found: C: 4.62; H, 3.49. IR (KBr, cm^{-1}): ν 3418(br, s), 1647(s), 1450(m), 1398(w), 1369(w), 1156(vs), 1133(vs), 975(vs), 929(m), 906(m), 818(m), 582(vs), 484(s). For **2**·Tb, Anal. Calcd for $C_4H_{20}O_{18}P_4Ru_2Tb\cdot 8H_2O$: C, 4.72; H, 3.54. Found: C: 4.76; H, 3.45. IR (KBr, cm^{-1}): ν 3416(br, s), 1647(s), 1450(m), 1400(w), 1369(w), 1148-(vs), 1121(vs), 975(vs), 930(m), 906(m), 813(m), 582(vs), 485(s). For **2**·Dy, Anal. Calcd for $C_4H_{20}O_{18}P_4Ru_2Dy\cdot 8H_2O$: C, 4.70; H, 3.53. Found: C: 4.84; H, 3.57. IR (KBr, cm^{-1}): ν 3421(br, s), 1638(s), 1449(m), 1398(w), 1369(w), 1149(vs), 1118(vs), 975(vs), 929(m), 906(m), 806(m), 580(vs), 481(s). For **2**·Ho, Anal. Calcd for $C_4H_{20}O_{18}P_4Ru_2Ho\cdot 8H_2O$: C, 4.69; H, 3.52. Found: C: 4.52; H, 3.58. IR (KBr, cm^{-1}): ν 3416(br, s), 1647(s), 1450(m), 1406-(w), 1369(w), 1150(vs), 1115(vs), 975(vs), 931(m), 906(m), 813-(m), 582(vs), 484(s). For **2**·Er, Anal. Calcd for $C_4H_{20}O_{18}P_4Ru_2Er\cdot 8H_2O$: C, 4.68; H, 3.51. Found: C: 4.53; H, 3.31. IR (KBr, cm^{-1}): ν 3417(br, s), 1645(s), 1450(m), 1395(w), 1369(w), 1153(vs), 977(vs), 929(m), 905(m), 814(m), 584(vs), 486(s).

Crystallographic Studies. Single crystals of dimensions 0.25 × 0.10 × 0.02 mm^3 for **1**·La, 0.30 × 0.10 × 0.05 mm^3 for **1**·Ce, 0.42 × 0.30 × 0.17 mm^3 for **2**·La, 0.12 × 0.10 × 0.10 mm^3 for **2**·Ce, 0.14 × 0.11 × 0.11 mm^3 for **2**·Pr, 0.13 × 0.10 × 0.08 mm^3 for **2**·Nd, 0.12 × 0.10 × 0.10 mm^3 for **2**·Gd, 0.20 × 0.15 × 0.15 mm^3 for **2**·Tb, 0.14 × 0.13 × 0.10 mm^3 for **2**·Dy, 0.22 × 0.15 × 0.13 mm^3 for **2**·Ho, and 0.22 × 0.15 × 0.10 mm^3 for **2**·Er were selected for indexing and intensity data collections on a Bruker SMART APEX CCD diffractometer at room temperature for **1**·Ln (Ln = La, Ce) and **2**·Ln (Ln = Pr, Tb, Ho, Er) or on a Rigaku Mercury CCD diffractometer at 193 K for **2**·Ln (Ln = La, Ce, Nd, Gd, Tb) using graphite-monochromatized Mo Kα radiation (λ = 0.71073 Å). The data were integrated using the Siemens SAINT[9] or CrystalClear program (Rigaku and MSC, version 3.60, 2004). Absorption corrections were applied. The structures were solved by direct methods and refined on F^2 by full-matrix least-squares using SHELXTL.[10] All non-hydrogen atoms were refined anisotropically. All the hydrogen atoms were either placed in calculated positions or located from the difference Fourier maps and refined isotropically. Crystallographic and refinement details are listed in Table 1, and the selected bond lengths and angles are listed in Tables 2 and 3.

Results and Discussion

Syntheses. Two synthetic routes A and B are employed in the preparation of compounds **1**·Ln and **2**·Ln. In route A, $Na_4[Ru_2(hedp)_2Cl]\cdot 16H_2O$ is used as the starting material. After removal of the Cl^- in $Na_4[Ru_2(hedp)_2Cl]$ through the precipitation of AgCl by $AgNO_3$, an aqueous solution of Ln-$(NO_3)_3$ is added to the filtrate. Brown amorphous solids deposit immediately. Such amorphous solids can be completely transformed into crystals of **1**·Ln or **2**·Ln when they are retained in the mother liquids for an extended period of time. By following this route, both **1**·Ln and **2**·Ln can be obtained when the lanthanide ions are La^{3+} and Ce^{3+}. For La^{3+}, **1**·La appears as a pure phase in 75% yield or, occasionally, contaminated with a very small amount of **2**·La. In the case of Ce^{3+}, **1**·Ce appears as a minor phase with a yield of ~2%. The major phase is **2**·Ce (yield ≈ 68%). When the lanthanide ions are Pr^{3+}, Nd^{3+}, Sm^{3+}, Eu^{3+}, Gd^{3+}, Tb^{3+}, Dy^{3+}, Ho^{3+}, and Er^{3+}, compounds **2**·Ln are obtained as single phases. It has to be noted that the removal of Cl^- is very important in the production **1**·Ln and **2**·Ln with good crystal qualities. Otherwise only amorphous solids together with some unrecognized polycrystalline materials are obtained, as judged by IR and powder XRD.

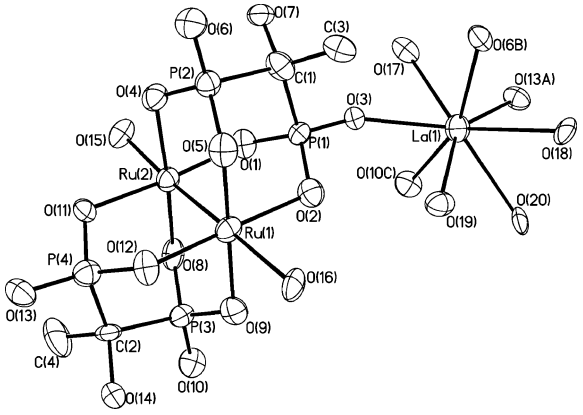

Figure 1. Building units of compound **1**·La with atomic labeling scheme (50% probability). All hydrogen atoms are omitted for clarity.

Scheme 1

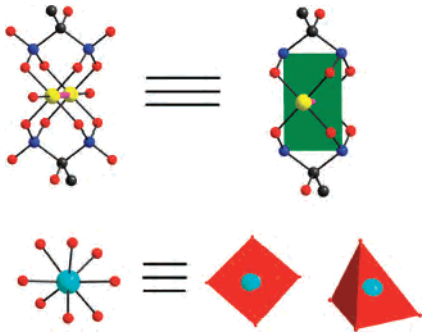

In route B, $(NH_4)_3[Ru_2(hedp)_2]\cdot 2H_2O$ is used as the starting material. This material can be dissolved in an aqueous solution of $LiNO_3$. The resulted solution, which is diluted to 2 × 10^{-4} M, is mixed with an aqueous solution of Ln-$(NO_3)_3$. Red brown block-shaped crystals appear after several days. By following this synthetic route, compounds **2**·Ln (Ln = La, Ce, Pr, Nd, Sm, Eu, Gd, Tb, Dy, Ho, Er) can be obtained as pure phases.

Crystal Structures of $Ln(H_2O)_4[Ru_2(hedp)_2(H_2O)_2]\cdot 4H_2O$ (1·Ln) [Ln = La, Ce]. Single-crystal structural analyses reveal that compounds **1**·La and **1**·Ce are isomorphous, crystallizing in monoclinic space group $P2_1/n$. Figure 1 shows the building unit of **1**·La with atomic labeling scheme. Clearly, a paddlewheel core of $Ru_2(hedp)_2(H_2O)_2^{3-}$ is observed. The Ru−O [2.024(5)−2.341(5) Å] and Ru−Ru [2.357(1) Å] distances in **1**·La are comparable to those in the other related complexes.[5] The $Ru_2(hedp)_2(H_2O)_2^{3-}$ core serves as donors and coordinates to four La^{3+} ions by using four phosphonate oxygen atoms (O3, O6, O10, and O13). Since these four phosphonate oxygen atoms are arranged approximately in the same plane, the $Ru_2(hedp)_2(H_2O)_2^{3-}$ unit

(9) *SAINT, Program for Data Extraction and Reduction*; Siemens Analytical X-ray Instruments Inc.; Madison, WI, 1994−1996.
(10) *SHELXTL*, version 5.0; Siemens Industrial Automation, Analytical Instrumentation: Madison, WI, 1995.

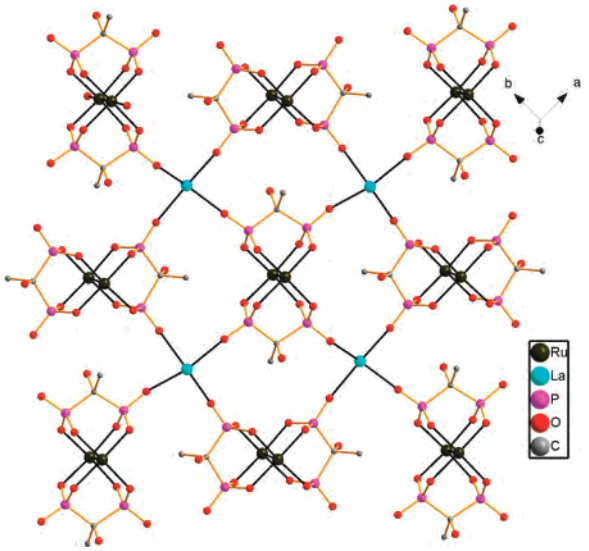

Figure 2. One layer of compound **1**·La viewed approximately along the *c*-axis. All hydrogen atoms and coordinated water molecules are omitted for clarity.

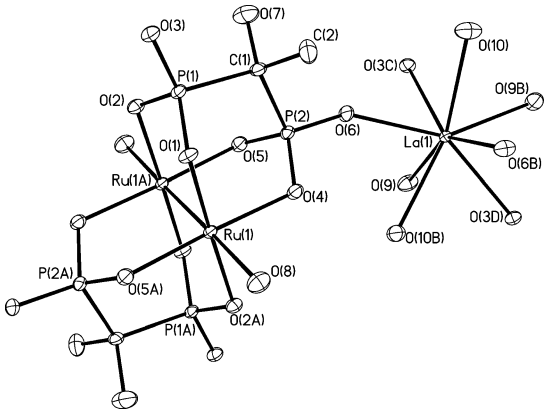

Figure 3. Building units of compound **2**·La with atomic labeling scheme (50% probability). All hydrogen atoms are omitted for clarity.

can be viewed as a tetradentate "ligand" which adopts a "rectangular" fashion of coordination (Scheme 1).

The local coordination geometry around the La1 center can be described as a distorted eight-coordinate square antiprism $LaO_{P4}O_{w4}$, where O_P represents phosphonate and O_w water oxygen atoms (Figure 1). The La−O_w bond lengths [2.522(6)−2.655(5) Å] are slightly longer than the La−O_P distances [2.370(5)−2.450(5) Å]. The O_P−La−O_P bond angles are 79.6(2), 86.4(2), 86.4(2), 92.7(2), 140.4(2), and 156.5(2)°. Hence, the LaO_{P4} unit can be approximately described as a distorted square plane (Scheme 1). The combination of $Ru_2(hedp)_2(H_2O)_2^{3-}$ rectangles and the LaO_{P4} planes leads to the formation of a square-grid layer structure in the *ab* plane (Figure 2). The lattice water molecules are stabilized between the layers through hydrogen-bond interactions.

Crystal Structures of $Ln(H_2O)_4[Ru_2(hedp)_2(H_2O)_2]\cdot 8H_2O$ (2·Ln) (Ln = La, Ce, Pr, Nd, Sm, Eu, Gd, Tb, Dy, Ho, Er). Compounds **2**·Ln are isomorphous, crystallizing in monoclinic space group *C*2/*c*. **2·La** will be used as an example. Figure 3 shows the building unit of compound **2**·La with atomic labeling scheme. The $Ru_2(hedp)_2(H_2O)_2^{3-}$ unit in **2**·La is analogous to that in **1**·La. The Ru−O and Ru−Ru distances are 2.026(2)−2.037(2) and 2.356(1) Å, respectively. It is again observed that the $Ru_2(hedp)_2(H_2O)_2^{3-}$ core is connected by four La^{3+} ions through four phosphonate oxygen atoms (O9, O9B, O10, and O10B) and vice versa. But the environment around the La atom is slightly different. In this case, the O_P−La1−O_P bond angles are 74.9(1), 74.9(1), 101.0(1), 130.4(1), 142.5(1), and 142.5(1)°. Hence the geometry of the LaO_{P4} unit is closer to being a distorted tetrahedron (Scheme 1). Accordingly, the combination of $Ru_2(hedp)_2(H_2O)_2^{3-}$ rectangles and LaO_{P4} tetrahedra results in an interesting PtS-type open framework,[11] in which the $Ru_2(hedp)_2(H_2O)_2^{3-}$ units occupy positions of Pt, while the LaO_{P4} units fill in the sites of S (Figure 4). The PtS-type framework structure was also observed in a monometallic compound, $Cu_2(ATC)\cdot 6H_2O$ (ATC = 1,3,5,7-adamantane tetracarboxylic acid), which contains Cu_2 paddlewheel cores.[12]

Three kinds of channels are generated within this framework structure, for example, channel A (4.3 × 3.5 Å) and channel B (3.6 × 4.9 Å) approximately along the [340] direction and channel C (3.5 × 3.5 Å) along the [001] direction (van der Waals radii are taken into account). The resultant free space is calculated to be 27% according to the PLATON program.[13] These spaces are filled with lattice water molecules. Four lattice water molecules (two O11 and two O13) form a cyclic water cluster through hydrogen bonds. Neighboring tetramers are further connected by coordinated water molecule (O8) through hydrogen bonds, forming water chains running along the [001] direction. The lattice water O12 is hydrogen bonded to the lattice water O14 and two coordinated water molecules (O9 and O10), forming another tetrameric water aggregates which are attached to the above-mentioned water chain through hydrogen-bond interactions between O8 and O14 (Supporting Information). Hydrogen-bond interactions are also found between O9 and the hydroxyl group O7, leading to the formation of a 3D network of hydrogen bonds.

Clearly, the structures of compounds **1**·Ln and **2**·Ln are completely different, although their compositions are very similar except for the number of lattice water molecules. When we look at these structures carefully, we find that both the bond lengths and angles within the $Ru_2(hedp)_2(H_2O)_2^{3-}$ unit are analogous in **1**·Ln and **2**·Ln. Significant differences are found in the bond angles of the $\{LnO_{P4}O_{w4}\}$ polyhedra. Since the $Ru_2(hedp)_2(H_2O)_2^{3-}$ units are connected by the lanthanide ions via phosphonate oxygen atoms (O_P) into two- or three-dimensional networks, the geometry of $\{LnO_{P4}\}$ becomes essential in determining the topologies of the final products. In the case of **1**·Ln, the geometry of $\{LnOp_4\}$ is closer to a distorted square plane. Accordingly, a square-grid layer structure is obtained through the combination of $Ru_2(hedp)_2(H_2O)_2^{3-}$ rectangles and the $\{LnO_{P4}\}$ planes. In

(11) Wells, A. F. *Three-dimensional Nets and Polyhedra*; Wiley: New York, 1977.
(12) Chen, B.; Eddaoudi, M.; Reineke, T. M.; Kampf, J. W.; O'Keeffe, M.; Yaghi, O. M. *J. Am. Chem. Soc.* **2000**, *122*, 11559−11560.
(13) Spek, A. L. *Acta Crystallogr.* **1990**, *A46*, C34.

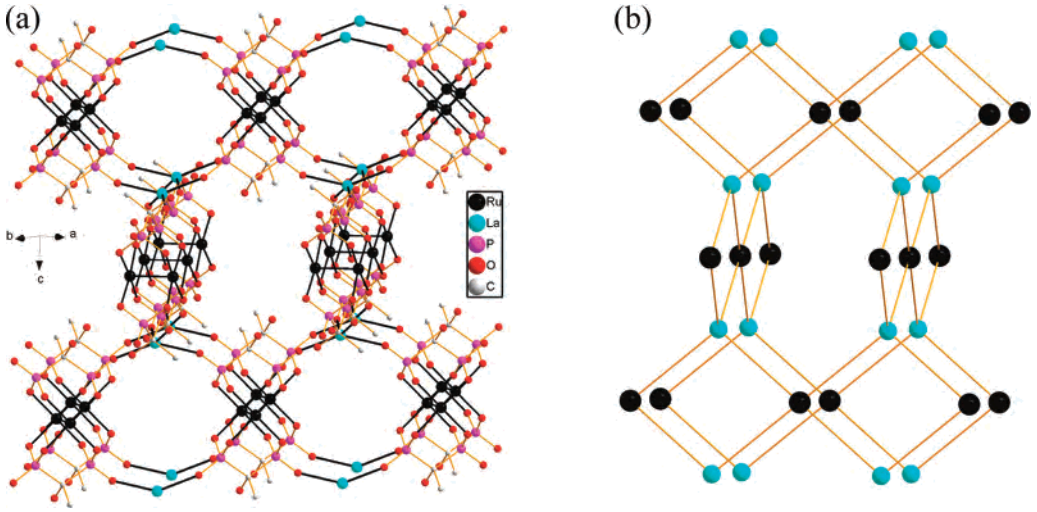

Figure 4. (a) Framework structure of compound **2**·La. All H atoms and water molecules are omitted for clarity. (b) A simplified view of the topology of **2**·La, where the centers of $Ru_2(hedp)_2^{3-}$ units are considered as nodes and O−P−O as linkers.

the case of **2**·Ln, the geometry of $\{LnO_{P4}\}$ is better described as a distorted tetrahedron. Consequently, the combination of $Ru_2(hedp)_2(H_2O)_2^{3-}$ rectangles and $\{LnO_{P4}\}$ tetrahedra results in a PtS-type open framework.

It would be of interest to find out which factors may influence the geometries of the $\{LnO_{P4}\}$ unit. As already described above, we use two synthetic routes in the preparation of compounds **1**·Ln and **2**·Ln. Synthetic route B results in compounds **2**·Ln as pure phases, while synthetic route A results in both **1**·Ln and **2**·Ln. Because the main difference between the two synthetic routes is the diruthenium source chosen as the starting material, either $Na_4[Ru_2(hedp)_2Cl]\cdot 16H_2O$ or $(NH_4)_3[Ru_2(hedp)_2]\cdot 2H_2O$, obviously a slight change of the synthetic condition could affect the geometry of the $\{LnO_{P4}\}$ unit and thus the structure of the final product. This is in agreement with the nature of coordination versatility and low stereochemical preference of the lanthanide ions. It is also noted that by employing the same synthetic route A, compounds **1**·Ln can be obtained only when the lanthanide ions are La^{3+} and Ce^{3+}. For the rest lanthanide ions, compounds **2**·Ln appear as pure phases. Therefore, the lanthanide contraction effect cannot be ruled out as well in the formation of structures **1**·Ln and **2**·Ln.

Thermal Analyses and Adsorption Properties. Thermal gravimetric analyses (TGA) are conducted to examine the stabilities of these compounds. For compound **1**·La, a weight loss (10.6%) in the temperature range of 20−90 °C corresponds to the release of 5.5 lattice water molecules (10.4%). The weight loss (12.2%) in the range of 90−350 °C is in agreement with the removal of six coordinated water molecules (11.7%). TG analysis for compound **2**·La shows a weight loss of 17.3% in the temperature range of 20−120 °C, corresponding to the release of eight lattice water molecules and two coordinated water molecules (18.1%). The weight loss (6.9%) in the range of 120−380 °C is in agreement with the calculated value for the removal of four coordinated water molecules (7.3%). The decomposition behaviors of **1**·Ce and **2**·Ln (Ln = Ce, Pr, Nd, Sm, Eu, Gd, Tb, Dy, Ho, Er) are similar to those of **1**·La and **2**·La, respectively (Supporting Information).

It is noted that the TG curves of compounds **2**·Ln show platforms up to ~450 °C after the removal of both lattice and coordinated water molecules. The XRD measurements, however, reveal that the framework structures of compounds **2**·Ln are not maintained after heat treatment above 150 °C. Adsorption properties of the partially dehydrated sample of **2**·La (heat treatment at 120 °C) are investigated with N_2. The surface area, determined using BET equation, is 4.87 m^2/g. Such a small surface area suggests that N_2 cannot diffuse into the channels of **2**·**La** after the removal of the lattice water molecules.

Magnetic Properties. The temperature-dependent magnetic susceptibilities for compounds **1**·Ln (Ln = La, Ce) and **2**·Ln (Ln = La, Ce, Pr, Nd, Sm, Eu, Gd, Tb, Dy, Ho, Er) were measured in the temperature range of 1.8−300 K (Figures 5−7). For **1**·La, the $\chi_M T$ value at 300 K is 2.32 $cm^3\ K\ mol^{-1}$ (4.31 μ_B per Ru_2^{5+} unit), corresponding to three unpaired electrons (Figure 5). Upon cooling of the sample, the $\chi_M T$ value decreases smoothly from 2.32 to 1.42 $cm^3\ K\ mol^{-1}$ (3.37 μ_B per dimer) at 1.8 K. Since the La^{3+} ion is diamagnetic, such a magnetic behavior is attributed to the large zero-field splitting (D) arising from the $S = 3/2$ ground state of Ru_2^{5+}. The magnetic susceptibility data can be analyzed by the equations described in the literature.[5b,7c] The best fit, shown as the solid line in Figure 7, results in parameters of $g = 2.24$, $D = 94.1\ cm^{-1}$, $zJ = -0.002\ cm^{-1}$, and TIP = $1.3 \times 10^{-4}\ cm^3\ mol^{-1}$, where zJ accounts for the magnetic exchange between the Ru_2^{5+} units. The magnetic behavior of compound **2**·La is similar to that of **1**·La. A monotonous decrease of the $\chi_M T$ value is again observed upon cooling of the sample from room temperature (2.33 $cm^3\ K\ mol^{-1}$) to 2.0 K (1.38 $cm^3\ K\ mol^{-1}$). The best fit, determined using similar equations, leads to parameters of $g = 2.23$, $D = 103.2\ cm^{-1}$, $zJ = -0.023\ cm^{-1}$ and TIP = $1.3 \times 10^{-4}\ cm^3\ mol^{-1}$ (Supporting Information).

For the other compounds, the room temperature $\chi_M T$ values are 2.96 $cm^3\ K\ mol^{-1}$ for **1**·Ce, 2.98 $cm^3\ K\ mol^{-1}$ for **2**·Ce, 3.75 $cm^3\ K\ mol^{-1}$ for **2**·Pr, 3.82 $cm^3\ K\ mol^{-1}$ for **2**·Nd, 2.74 $cm^3\ K\ mol^{-1}$ for **2**·Sm, 3.74 $cm^3\ K\ mol^{-1}$ for **2**·Eu, 10.28 $cm^3\ K\ mol^{-1}$ for **2**·Gd, 13.84 $cm^3\ K\ mol^{-1}$ for **2**·Tb,

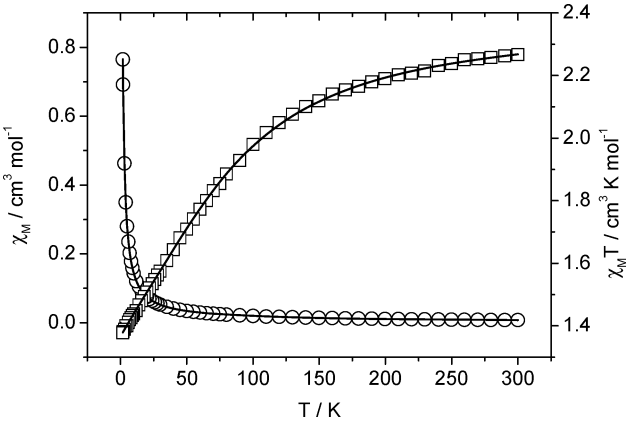

Figure 5. χ_M and $\chi_M T$ vs T plots for compound **1**·La.

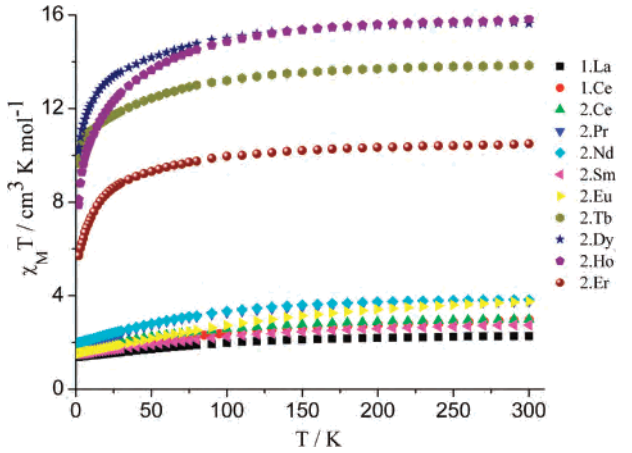

Figure 6. $\chi_M T$ vs T plots for compounds **1**·Ln (Ln = La, Ce) and **2**·Ln (Ln = Ce, Pr, Nd, Sm, Eu, Gd, Tb, Dy, Ho, Er).

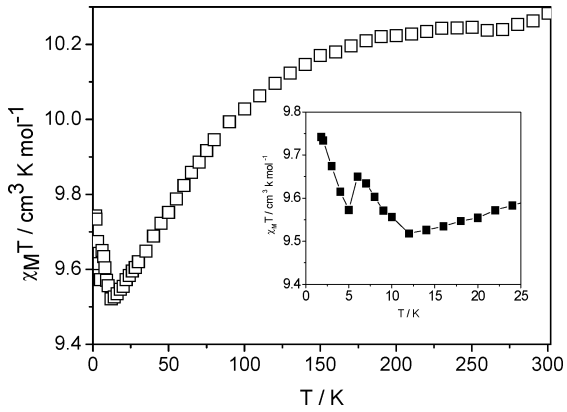

Figure 7. $\chi_M T$ vs T plot for compound **2**·Gd.

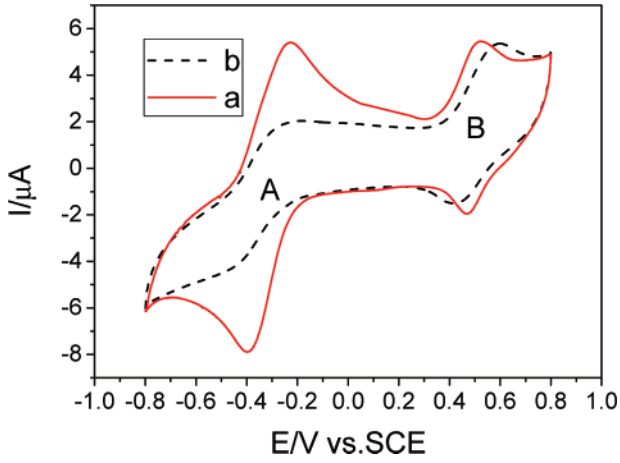

Figure 8. Cyclic voltammograms of (a) **1**·La/GC and (b) **2**·La/GC electrodes in 0.5 M KNO_3 solution at a scan rate of 0.10 V/s.

15.64 cm^3 K mol^{-1} for **2**·Dy, 15.83 cm^3 K mol^{-1} for **2**·Ho, and 13.78 cm^3 K mol^{-1} for **2**·Er, respectively (Figure 6). With a paramagnetic contribution from the diruthenium unit of 2.32 cm^3 K mol^{-1}, the contributions per lanthanide ion, calculated by the equation $(\chi_M T)_{Ln} = (\chi_M T)_{total} - (\chi_M T)_{Ru2}$, are 0.64 cm^3 K mol^{-1} for Ce^{3+} in **1**·Ce, 0.66 cm^3 K mol^{-1} for Ce^{3+} in **2**·Ce, 1.43 cm^3 K mol^{-1} for Pr^{3+}, 1.50 cm^3 K mol^{-1} for Nd^{3+}, 0.42 cm^3 K mol^{-1} for Sm^{3+}, 1.42 cm^3 K mol^{-1} for Eu^{3+}, 7.96 cm^3 K mol^{-1} for Gd^{3+}, 11.52 cm^3 K mol^{-1} for Tb^{3+}, 13.32 cm^3 K mol^{-1} for Dy^{3+}, 13.51 cm^3 K mol^{-1} for Ho^{3+}, and 11.46 cm^3 K mol^{-1} for Er^{3+}. These values are fairly close to the typical values for the free lanthanide ions except for those of Sm^{3+} and Eu^{3+}.[2b] In the latter cases, the $\chi_M T$ are larger than the expected values because of the presence of thermally populated excited states of Sm^{3+} and Eu^{3+}.

Upon cooling of the sample to 1.8 K, the $\chi_M T$ values decrease continuously in all cases except for that for **2**·Gd (Figure 7). Such a magnetic behavior could be attributed to the large zero-field splitting of Ru_2^{5+} species, the thermal depopulations of the Stark levels of the lanthanide ions, and the weak antiferromagnetic interactions between paramagnetic centers Ru_2^{5+} and Ln^{3+}. For compound **2**·Gd, a minimum of 9.52 cm^3 K mol^{-1} is found at 12 K, below which $\chi_M T$ increases until it approaches 9.65 cm^3 K mol^{-1} at 6 K. When the temperature is lower than 6 K, the $\chi_M T$ value drops to 9.57 cm^3 K mol^{-1} at 5 K and then increases again below 5 K (Figure 7, inset). Such magnetic behavior could be related to a weak ferromagnetic exchange between the magnetic centers. The mechanism is, however, not clear to us.

Electrochemical Properties. The electrochemical properties of compounds **1**·La and **2**·La deposited on a glassy carbon (GC) electrode are investigated. Figure 8 shows the cyclic voltammograms of **1**·La/GC and **2**·La/GC electrodes in 0.5 M KNO_3 solution for the second cycle. Clearly, solid state **1**·La or **2**·La shows two couples of redox peaks in the cyclic voltammograms. For **1**·La, one couple of redox peaks is located at −228 and −397 mV, and another couple is located at 524 and 467 mV, respectively (Figure 8, curve a). Theu differences of their anodic and cathodic peak potentials, ΔE_p, are 169 and 57 mV, respectively. The anodic peak current is almost equal to the cathodic peak current for both couples of redox peaks. The above results illustrate that the electrochemical reaction of **1**·La is quasireversible. The formal redox potentials, $E_{1/2}$, are −313 and 495 mV. The electrochemical reaction of **1**·La at −313 mV is attributed to the reduction of Ru_2^{5+}/Ru_2^{4+} (A) and the one at 495 mV to the oxidation of Ru_2^{5+}/Ru_2^{6+} (B). For **2**·La, the anodic and cathodic peaks are located at −238, 596, −428, and 408 mV, respectively (Figure 8, curve b). Their ΔE_p values are 190 and 188 mV, respectively. The anodic peak current is

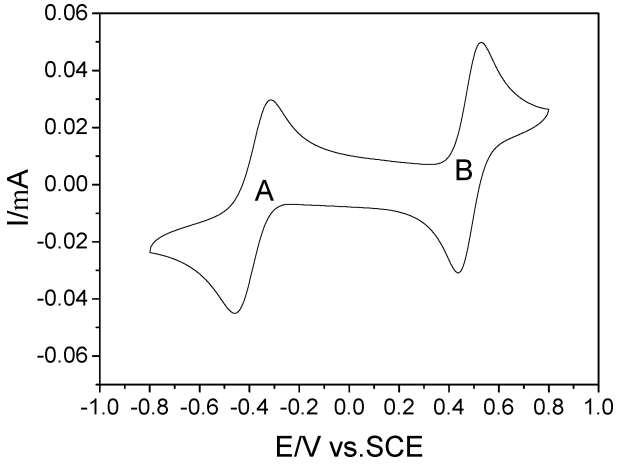

Figure 9. Cyclic voltammograms of bare GC electrode in 0.5 M KNO_3 solution containing 5 mM $Na_4[Ru_2(hedp)_2Cl]\cdot 16H_2O$ at a scan rate of 0.10 V/s.

Table 4. Redox Properties for **1**·La, **2**·La, and $Na_4[Ru_2(hedp)_2Cl]\cdot 16H_2O$[a]

	reduction (A)				oxidation (B)			
compound	E_{paA} (mV)	E_{pcA} (mV)	$E_{1/2A}$ (mV)	ΔE_{pA} (mV)	E_{paB} (mV)	E_{pcB} (mV)	$E_{1/2B}$ (mV)	ΔE_{pB} (mV)
1·La	−228	−397	−313	169	524	467	495	57
2·La	−238	−428	−333	190	596	408	502	188
$Na_4[Ru_2(hedp)_2Cl]\cdot 16H_2O$	−314	−460	−387	146	529	437	483	92

[a] E_{pa} = anodic peak potential; E_{pc} = cathodic peak potential; $E_{1/2} = {}^1/_2(E_{pa} + E_{pc})$; $\Delta E_P = E_{pa} - E_p$).

almost equal to the cathodic peak current for both couples of the redox peaks. The above results illustrate that the electrochemical reaction of the **2**·La compound is also quasi-reversible. Redox properties for the **1**·La and **2**·La compounds are listed in Table 4.

As is well-known, more than one couple of redox peaks can appear in the cyclic voltammograms of diruthenium compounds in solution.[14] The observation of the Ru_2^{5+}/Ru_2^{6+} redox couple is, however, not common for diruthenium tetra-bridged species with carboxylate and other oxy ligands. The only report, as far as we are aware, is concerned with compound $[Ru_2(\mu\text{-}O_2CCH_3)_4(PCy_3)_2](PF_6)$ (PCy_3 = tris-(cyclohexyl)phosphine), in which the strong Lewis base PCy_3 occupies the axial positions of the Ru_2 species.[15] This compound shows a very long Ru−Ru bond length [2.427-(1)Å] and provides access to the Ru_2^{5+}/Ru_2^{6+} redox couple.[15]

One question arising from Figure 8 is that the peak current of couple B is much smaller than that of A for **1**·La. They should be comparable if both are 1e couples. To clarify this question, we analyzed the CV of one parent complex $Na_4[Ru_2(hedp)_2Cl]\cdot 16H_2O$, which is displayed in Figure 9. Apparently, the peak currents of the two couples of this compound are indeed comparable, confirming the assignments of the Ru_2^{5+}/Ru_2^{4+} and Ru_2^{5+}/Ru_2^{6+} couples. The smaller peak current of couple B than that of couple A for compound **1**·La could be caused by the involvement of the lanthanide ions in the structure, the reason of which is still not clear to us. Further, the electrochemical reaction of **1**·La, shown from Table 4 and Figure 8, seems to be more reversible than that of **2**·La. Because the active center and the ligand of two diruthenium compounds are the same, their difference of the electrochemical reactions can only be attributed to the difference in their crystal structures.

Conclusion. In this paper, we report the first Ln−Ru_2 compounds through self-assembly of preformed $Ru_2(hedp)_2^{3-}$ and Ln^{3+} ions in aqueous solutions by following two synthetic routes. Compounds $Ln(H_2O)_4[Ru_2(hedp)_2(H_2O)_2]\cdot 5.5H_2O$ (**1**·Ln, Ln = La, Ce) have a square-grid layer structure, in which the $Ru_2(hedp)_2(H_2O)_2^{3-}$ rectangles are linked by the $\{LaO_{P4}\}$ planes. While compounds $Ln(H_2O)_4[Ru_2(hedp)_2(H_2O)_2]\cdot 8H_2O$ (**2**·Ln, Ln = La, Ce, Pr, Nd, Sm, Eu, Gd, Tb, Dy, Ho, Er) display a unique PtS-type open-framework structure, where the $Ru_2(hedp)_2(H_2O)_2^{3-}$ rectangles are combined with the $\{LaO_{P4}\}$ tetrahedra. The results demonstrate that extended lanthanide−Ru_2 heterometallic frameworks with desired topologies can be achieved through the simple building block approach under suitable experimental conditions. Further work is in progress to extend this approach to the other systems.

Acknowledgment. We thank the National Natural Science Fund for Distinguished Young Scholars (20325103) and the specialized research fund for the doctoral program of the Ministry of Education of China (20040284004) and the National Basic Research Program of China (2007CB925102) for financial supports and Prof. S. Kitagawa and Prof. Z.-G. Zou for kind help, Mr. Yong-Jiang Liu and Mr. Yong Zhang for crystal data collection, and Prof. You Song and Prof. De-qing Zhang for magnetic measurements.

Supporting Information Available: X-ray crystallographic files in CIF format, structure of the water chain in **2**·La,TG curves for all compounds, XRD patterns of compound **2**·La before and after heat treatments, and the χ_M and $\chi_M T$ versus **T** plots for **2**·La. This material is available free of charge via the Internet at http://pubs.acs.org. CCDC 622677−622687 contain the supplementary crystallographic data for this paper. These data can be obtained free of charge via www.ccdc.cam.ac.uk/conts/retrieving.html (or from the Cambridge Crystallographic Data Center, 12, Union Road, Cambridge CB21EZ, UK; fax: (+44) 1223−336-033; e-mail: deposit@ccdc.cam.ac.uk).

IC0621695

(14) (a) Chen, W. Z.; Ren, T. *Inorg. Chem.* **2006**, *45*, 8156. (b) Blum, A. S.; Ren, T.; Parish, D. A.; Trammell, S. A.; Moore, M. H.; Kushmerick, J. G.; Xu, G. L.; Deschamps, J. R.; Pollack, S. K.; Shashidhar, R. J. *Am. Chem. Soc.* **2005**, *127*, 10010. (c) Xu, G. L.; Wang, C. Y.; Ni, Y. H.; Goodson, T. G.; Ren, T. *Organometallics* **2005**, *24*, 3247. (d) Angaridis, P.; Cotton, F. A.; Murillo, C. A.; Villagran, D.; Wang, X. *Inorg. Chem.* **2004**, *43*, 8290. (e) Kadish, K. M.; Wang, L. L.; Thuriere, A.; Giribabu, L.; Garcia, R.; Van Caemelbecke, E.; Bear, J. L. *Inorg. Chem.* **2003**, *42*, 8309. (f) Hurst, S. K.; Xu, G. L.; Ren, T. *Organometallics* **2003**, *22*, 4118. (g) Cotton, F. A.; Yokochi, A. *Inorg. Chem.* **1998**, *37*, 2723. (h) Shen, H. F.; Bott, S. G.; Richmond, M. G. *Organometallics* **1995**, *14*, 4625. (i) Malinski, T.; Chang, D.; Feldmann, F. N.; Bear, J. L.; Kadish, K. M. *Inorg. Chem.* **1983**, *22*, 3225.

(15) Briand, G. G.; Cooke, M. W.; Cameron, T. S.; Farrell, H. M.; Burchell, T. J.; Aquino, M. A. S. *Inorg. Chem.* **2001**, *40*, 3267.